- When Does Carbonylation of Carbenes Yield Ketenes? A Theoretical Study with Implications for Synthesis
  Goedecke, C.; Leibold, M.; Siemeling, U.; Frenking, G. *J. Am. Chem. Soc.* **2011***, 133*, 3557–3569.
  Abstract:

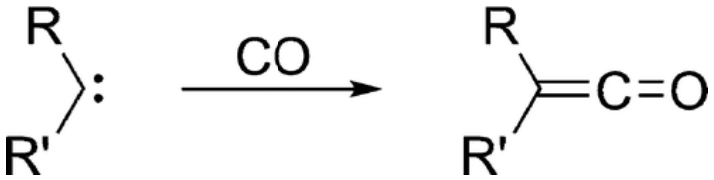

Quantum-chemical calculations using DFT and ab initio methods have been carried out for 32 carbenes RR□C which comprise different classes of compounds and the associated ketenes RR□C═C═O. The calculated singlet−triplet gaps ΔE_{S-T} of the carbenes exhibit a very high correlation with the bond dissociation energies (BDEs) of the ketenes. An energy decomposition analysis of the RR□C−CO bond using the triplet states of the carbene and CO as interacting fragments supports the assignment of ΔE_{S-T} as the dominant factor for the BDE but also shows that the specific interactions of the carbene may sometimes compensate for the S/T gap. The trend of the interaction energy ΔE_{int} values is mainly determined by the Pauli repulsion between the carbene and CO. The stability of amino-substituted ketenes strongly depends on the destabilizing conjugation between the nitrogen lone-pair orbital and the ketene double bonds. There is a ketene structure of the unsaturated N-heterocyclic carbene parent compound **NHC1** with CO as a local energy minimum on the potential-energy surface. However, the compound **NHC1−CO** is thermodynamically unstable toward dissociation. The saturated homologue **NHC2−CO** has only a very small bond dissociation energy of D_e = 3.2 kcal/mol. The [3]ferrocenophane-type compound **FeNHC−CO** has a BDE of D_e = 16.0 kcal/mol.

- Impact of Water on the OH + HOCl Reaction
  Gonzalez, J.; Anglada, J. M.; Buszek, R. J.; Francisco, J. S. *J. Am. Chem. Soc.* **2011**, *133*, 3345–3353.
  Abstract:

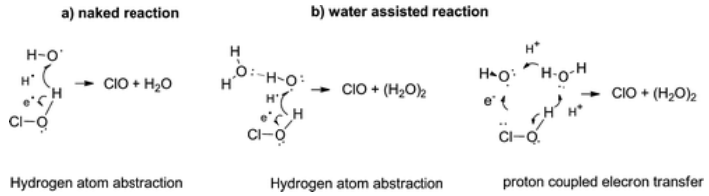

The effect of a single water molecule on the OH + HOCl reaction has been investigated. The naked reaction, the reaction without water, has two elementary reaction paths, depending on how the hydroxyl radical approaches the HOCl molecule. In both cases, the reaction begins with the formation of prereactive hydrogen bond complexes before the abstraction of the hydrogen by the hydroxyl radical. When water is added, the products of the reaction do not change, and the reaction becomes quite complex yielding six different reaction paths. Interestingly, a geometrical rearrangement occurs in the prereactive hydrogen bonded region, which prepares the HOCl moiety to react with the hydroxyl radical. The rate constant for the reaction without water is computed to be 2.2×10^{-13} cm^3 molecule^{-1} s^{-1} at room temperature, which is in good agreement with experimental values. The reaction between ClOH···H_2O and OH is estimated to be slower than the naked reaction by 4−5 orders of magnitude. Although, the reaction between ClOH and the H_2O···HO complex is also

predicted to be slower, it is up to 2.2 times faster than the naked reaction at altitudes below 6 km. Another intriguing finding of this work is an interesting three-body interchange reaction that can occur, that is HOCl + HO···H_2O → HOCl···H_2O + OH.

- Tetrathienoanthracene-Based Copolymers for Efficient Solar Cells
  He, F.; Wang, W.; Chen, W.; Xu, T.; Darling, S. B.; Strzalka, J.; Liu, Y.; Yu, Y. *J. Am. Chem. Soc.* **2011**, *133*, 3284–3287.
  Abstract:

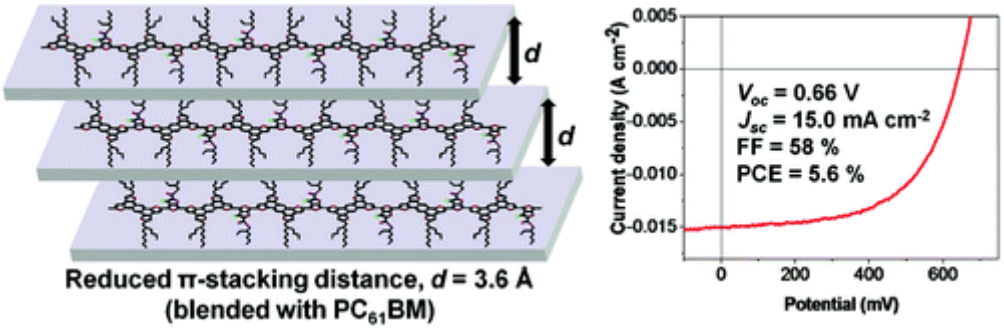

A series of semiconducting copolymers (PTAT-x) containing extended π-conjugated tetrathienoanthracene units have been synthesized. It was shown that the extended conjugation system enhanced the π–π stacking in the polymer/PC61BM blend films and facilitated the charge transport in heterojunction solar cell devices. After structural fine-tuning, the polymer with bulky 2-butyloctyl side chains (PTAT-3) exhibited a PCE of 5.6% when it was blended with PC61BM.

- Controlled Intramolecular Electron Transfers in Cyanide-Bridged Molecular Squares by Chemical Modifications and External Stimuli
  Nihei, M.; Sekine, Y.; Suganami, N.; Nakazawa, K.; Nakao, A.; Nakao, H.; Murakami, Y.; Oshio, H. *J. Am. Chem. Soc.* **2011**, *133*, 3592–3600.
  Abstract:

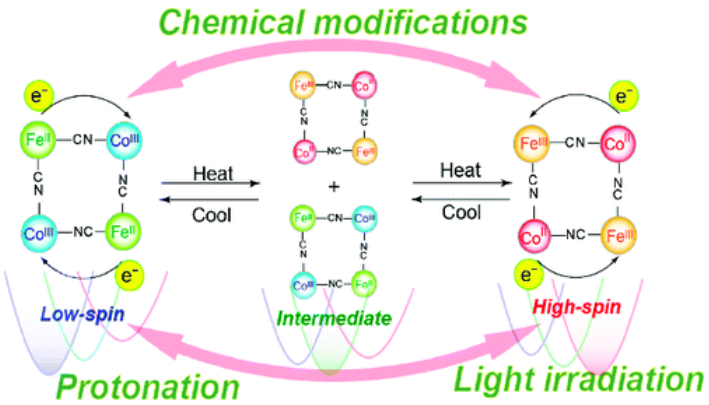

A series of cyanide bridged Fe–Co molecular squares, [Co2Fe2(CN)6(tp*)2(dtbbpy)4](PF6)2·2MeOH (1), [Co2Fe2(CN)6(tp*)2(bpy)4](PF6)2·2MeOH (2), and [Co2Fe2(CN)6(tp)2(dtbbpy)4](PF6)2·4H2O (3) (tp = hydrotris(pyrazol-1-yl)borate, tp* = hydrotris(3,5-dimethylpyrazol-1-yl)borate, bpy =2,2′-bipyridine, dtbbpy =4,4′-di-tert-butyl-2,2′-bipyridine), were prepared by the reactions of [Fe(CN)3(L)]− (L = tp or tp*) with Co2+ and bidentate ligands (bpy or dtbbpy) in MeOH. In the molecular squares, Fe and Co ions are alternately bridged by cyanide ions, forming macrocyclic tetranuclear cores. Variable temperature X-ray structural analyses and magnetic susceptibility measurements confirmed that 1 exhibits two-step charge-transfer induced spin transitions (CTIST)

centered at T1/2 = 275 and 310 K in the solid state. The Fe and Co ions in 1 are the low-spin (LS) Fe(III) and high-spin (HS) Co(II) ions, described here in the high-temperature (HT) phase ([FeIIILS2CoIIHS2]) at 330 K, while a low-temperature (LT) phase ([FeIILS2CoIIILS2]) with LS Fe(II) and Co(III) ions was dominant below 260 K. X-ray structural analysis revealed that in the intermediate (IM) phase at 298 K 1 exhibits positional ordering of [FeIIILS2CoIIHS2] and [FeIILS2CoIIILS2] species with the 2:2 ratio. In photomagnetic experiments on 1, light-induced CTIST from the LT to the HT phase was observed by excitation of Fe(II) → Co(III) intervalence charge transfer (IVCT) band at 5 K and the trapped HT phase thermally relaxed to the LT phase in a two-step fashion. On the other hand, 2 and 3 are in the HT and LT phases, respectively, throughout the entire temperature range measured, and no CTIST was observed. UV−vis-NIR absorption spectral measurements and cyclic voltammetry in solution revealed that the different electronic states in 1−3 are ascribable to the destabilization of iron and cobalt ion d-orbitals by the introduction of methyl and tert-butyl groups to the ligands tp and bpy, respectively. Temperature dependence of UV−vis-NIR spectra confirmed that 1 exhibited a one-step CTIST in butyronitrile, of which T1/2 varied from 227 to 280 K upon the addition of trifluoroacetic acid.

- DNA charge transport over 34 nm
  Slinker, J. D.; Muren, N. B.; Renfrew, S. E.; Barton, J. K. *Nature Chemistry* **2011**, *3*, 230–235.
  Abstract:

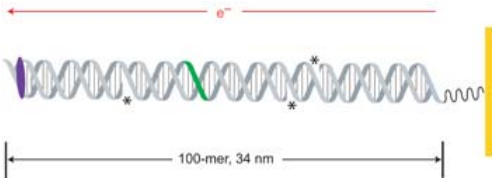

Molecular wires show promise in nanoscale electronics, but the synthesis of uniform, long conductive molecules is a significant challenge. Deoxyribonucleic acid (DNA) of precise length, by contrast, is synthesized easily, but its conductivity over the distances required for nanoscale devices has not been explored. Here we demonstrate DNA charge transport (CT) over 34 nm in 100-mer monolayers on gold. Multiplexed gold electrodes modified with 100-mer DNA yield sizable electrochemical signals from a distal, covalent Nile Blue redox probe. Significant signal attenuation upon incorporation of a single base-pair mismatch demonstrates that CT is DNA-mediated. Efficient cleavage of these 100-mers by a restriction enzyme indicates that the DNA adopts a native conformation accessible to protein binding. Similar electron-transfer rates measured through 100-mer and 17-mer monolayers are consistent with rate-limiting electron tunnelling through the saturated carbon linker. This DNA-mediated CT distance of 34 nm surpasses that of most reports of molecular wires.

- Creating Favorable Geometries for Directing Organic Photoreactions in Alkanethiolate Monolayers
  Kim, M.; Hohman, J. N.; Cao, Y.; Houk, K. N.; Ma, H.; Jen, A. K.-Y.; Weiss, P. S. *Science* **2011**, *331*, 1312-1315.
  Abstract:

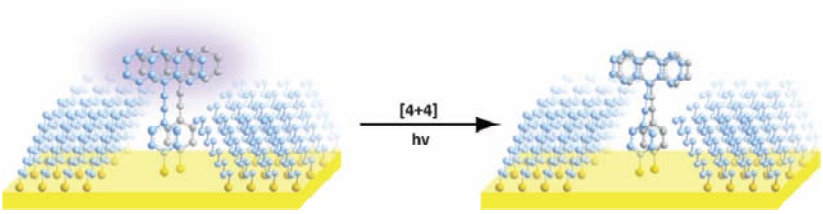

The products of photoreactions of conjugated organic molecules may be allowed by selection rules but not observed in solution reactions because of unfavorable reaction geometries. We have used defect sites in self-assembled alkanethiolate monolayers on gold surfaces to direct geometrically unfavorable photochemical reactions between individual organic molecules. High conductivity and stochastic switching of anthracene-terminated phenylethynylthiolates within alkanethiolate monolayers, as well as in situ photochemical transformations, have been observed and distinguished with the scanning tunneling microscope (STM). Ultraviolet light absorbed during imaging increases the apparent heights of excited molecules in STM images, a direct manifestation of probing electronically excited states.

- Vertical nanopillars for highly localized fluorescence imaging
  Xie, C.; Hanson, L.; Cui, Y.; Cui, B. *Proc. Nat. Acad. Sci.* **2011**, *108*, 3894-3899.
  Abstract:

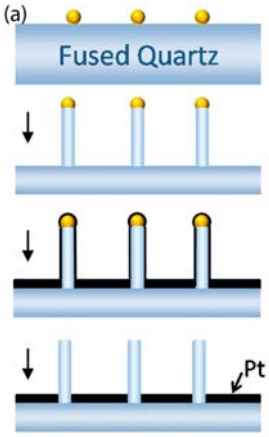

Observing individual molecules in a complex environment by fluorescence microscopy is becoming increasingly important in biological and medical research, for which critical reduction of observation volume is required. Here, we demonstrate the use of vertically aligned silicon dioxide nanopillars to achieve below-the-diffraction-limit observation volume in vitro and inside live cells. With a diameter much smaller than the wavelength of visible light, a transparent silicon dioxide nanopillar embedded in a nontransparent substrate restricts the propagation of light and affords evanescence wave excitation along its vertical surface. This effect creates highly confined illumination volume that selectively excites fluorescence molecules in the vicinity of the nanopillar. We show that this nanopillar illumination can be used for in vitro single-molecule detection at high fluorophore concentrations. In addition, we demonstrate that vertical nanopillars interface tightly with live cells and function as highly localized light sources inside the cell. Furthermore, specific chemical modification of the nanopillar surface makes it possible to locally recruit proteins of interest and simultaneously observe their behavior within the complex, crowded environment of the cell.

- A Programmable Molecular Robot
  Muscat, R. A.; Bath, J.; Turberfield, A. J. *Nano Lett.* **2011**, *11*, 982–987.

Abstract:

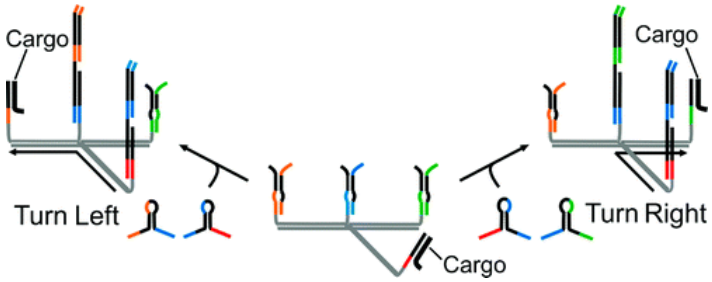

We have developed a programmable and autonomous molecular robot whose motion is fueled by DNA hybridization. Instructions determining the path to be followed are programmed into the fuel molecules, allowing precise control of cargo motion on a branched track.

- Synthesis and Growth Mechanism of Iron Oxide Nanowhiskers
  Palchoudhury, S.; An, W.; Xu, Y.; Qin, Y.; Zhang, Z.; Chopra, N.; Holler, R. A.; Turner, C. H.; Bao, Y. *Nano Lett.* **2011**, *11*, 1141–1146.
  Abstract:

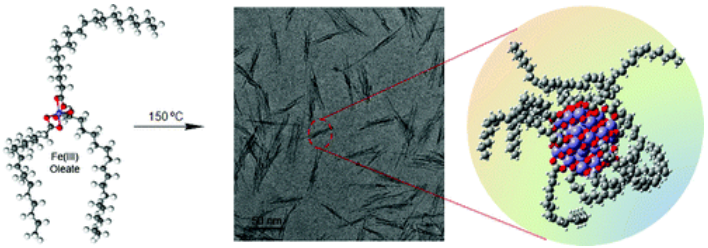

Iron oxide nanowhiskers with dimensions of approximately 2 × 20 nm were successfully synthesized by selectively heating an iron oleate complex. Such nanostructures resulted from the difference in the ligand coordination microenvironments of the Fe(III) oleate complex, according to our electronic structure calculations and thermogravimetric analysis. A ligand-directed growth mechanism was subsequently proposed to rationalize the growth process. The formation of the nanowhiskers provides a unique example of shape-controlled nanostructures, offering additional insights into nanoparticle synthesis.

- Lewis Acid-Mediated Michaelis–Arbuzov Reaction at Room Temperature: A Facile Preparation of Arylmethyl/Heteroarylmethyl Phosphonates
  Rajeshwaran, G. G.; Nandakumar, M.; Sureshbabu, R.; Mohanakrishnan, A. K. *Org. Lett.* **2011**, *13*, 1270–1273.
  Abstract:

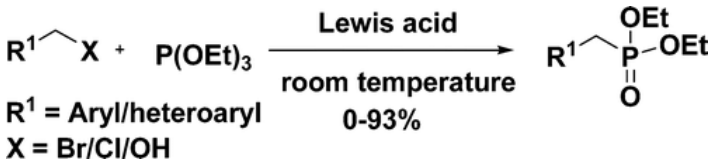

A facile preparation of arylmethyl and heteroarylmethyl phosphonate esters was achieved involving a Lewis acid mediated Michaelis–Arbuzov reaction at room temperature. Interaction of arylmethyl halides/alcohols with triethyl phosphite in the presence of Lewis acid at room temperature afforded phosphonate esters in good yields.

- Cu-Catalyzed One-Pot Synthesis of Unsymmetrical Diaryl Thioethers by Coupling of Aryl Halides Using a Thiol Precursor
  Prasad, D. J. C.; Sekar, G. *Org. Lett.* **2011**, *13*, 1008–1011.
  Abstract:

An efficient Cu-catalyzed one-pot approach for the synthesis of unsymmetrical diaryl thioethers using potassium ethyl xanthogenate as a thiol surrogate is developed. This new protocol avoids usage of intricate thiols and makes use of its easily available xanthate as a precursor, and thiol will be generated *in situ* to prepare the diaryl thioethers through a Cu-catalyzed double arylation. This strategy was further successfully utilized for the synthesis of symmetrical diaryl thioethers, aryl alkyl thioethers, and benzothiazoles.

- One-Pot Triple Functionalization of Carbon Nanotubes
  Ménard-Moyon, C.; Fabbro, C.; Prato, M.; Bianco, A. *Chem.-Eur. J.* **2011**, *17*, 3222-3227.
  Abstract:

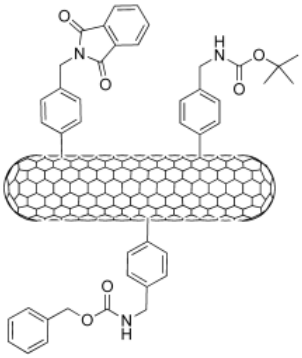

Carbon nanotubes (CNTs) are very promising as carriers for the delivery of bioactive molecules. The multifunctionalization of CNTs is necessary to impart multimodalities for the development of future CNT-based multipotent therapeutic constructs. In this context, we report the first example of covalent trifunctionalization of different types of CNTs. Our strategy is a simple and efficient methodology based on the simultaneous functionalization of the nanotube surface with three different active groups. The reaction is performed in one step by arylation with diazonium salts generated in situ. The CNTs are functionalized with benzylamine moieties blocked with three different protecting groups that can be selectively removed under specific conditions. The trifunctionalized CNTs were characterized by TEM, thermogravimetric analysis, and Raman and UV/Vis/NIR spectroscopy, while the amine loading was determined by using the Kaiser test. The sequential removal of the protecting groups of the amine functions allows the grafting of the molecules of interest on the nanotube surface to be controlled.

- From Molecular to Macroscopic Engineering: Shaping Hydrogen-Bonded Organic Nanomaterials
  Yoosaf, K.; Llanes-Pallas, A.; Marangoni, T.; Belbakra, A.; Marega, R.; Botek, E.; Champagne, B.; Bonifazi, D.; Armaroli, N. *Chem.-Eur. J.* **2011**, *17*, 3262-3273.
  Abstract:

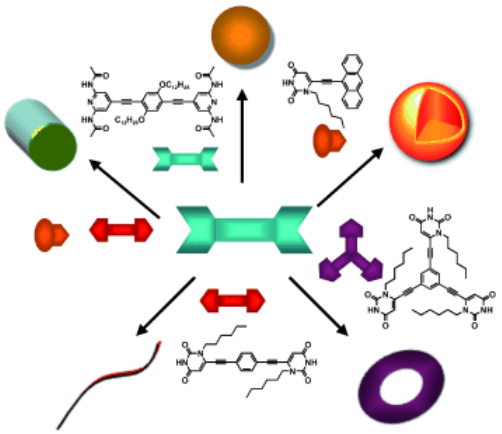

The self-assembly and self-organization behavior of chromophoric acetylenic scaffolds bearing 2,6-bis(acetylamino)pyridine (**1**, **2**) or uracyl-type (**3**–**9**) terminal groups has been investigated by photophysical and microscopic methods. Systematic absorption and luminescence studies show that **1** and **2**, thanks to a combination of solvophilic/solvophobic forces and π–π stacking interactions, undergo self-organization in apolar solvents (i.e., cyclohexane) and form spherical nanoparticles, as evidenced by wide-field optical microscopy, TEM, and AFM analysis. For the longer molecular module, **2**, a more uniform size distribution is found (80–200 nm) compared to **1** (20–1000 nm). Temperature scans in the range 283–353 K show that the self-organized nanoparticles are reversibly formed and destroyed, being stable at lower temperatures. Molecular modules **1** and **2** were then thoroughly mixed with the complementary triply hydrogen-bonding units **3**–**9**. Depending on the specific geometrical structure of **3**–**9**, different nanostructures are evidenced by microscopic investigations. Combination of modules **1** or **2** with **3**, which bears only one terminal uracyl unit, leads to the formation of vesicular structures; instead, when **1** is combined with bis-uracyl derivative **4** or **5**, a structural evolution from nanoparticles to nanowires is observed. The length of the wires obtained by mixing **1** and **4** or **1** and **5** can be controlled by addition of **3**, which prompts transformation of the wires into shorter rods. The replacement of linear system **5** with the related angular modules **6** and **7** enables formation of helical nanostructures, unambiguously evidenced by AFM. Finally, thermally induced self-assembly was studied in parallel with modules **8** and **9**, in which the uracyl recognition sites are protected with *tert*-butyloxycarbonyl (BOC) groups. This strategy allows further control of the self-assembly/self-organization process by temperature, since the BOC group is completely removed on heating. Microscopy studies show that the BOC-protected ditopic modules **8** self-assemble and self-organize with **1** into ordered linear nanostructures, whereas BOC-protected tritopic system **9** gives rise to extended domains of circular nano-objects in combination with **1**.

- Two-Dimensional Nanostructures from Positively Charged Polycyclic Aromatic Hydrocarbons
  Wu, D.; Liu, R.; Pisula, W.; Feng, X.; Müllen, K. *Angew. Chem. Int. Ed.* **2011**, *50*, 2791-2794.
  Abstract:

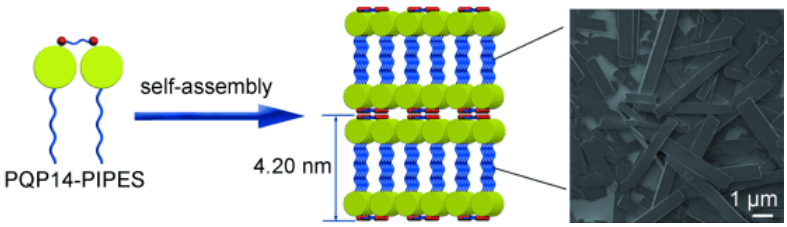

Conducting experiments: Amphiphilic PQP14 complexes self-assemble into two-dimensional (2D) nanostructures in a controlled way by choosing alkyl sulfonates or disulfonates as anions (see picture). The morphologies of these 2D nanostructures significantly affect the ionic conductivity of the mixture of PQP14 complexes and lithium salts, for which the planar aggregates exhibit a conductivity of two orders of magnitude higher than that of the puckered ones.

- All-Polymer Solar Cells from Perylene Diimide Based Copolymers: Material Design and Phase Separation Control
  Zhou, E.; Cong, J.; Wei, Q.; Tajima, K.; Yang, C.; Hashimoto, K. *Angew. Chem. Int. Ed.* **2011**, *50*, 2799-2803.
  Abstract:

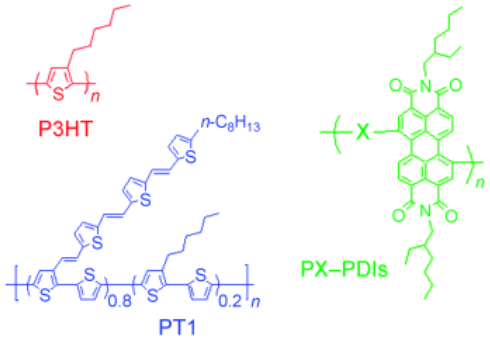

It's all about polymers: All-polymer solar cells (all-PSCs) based on six perylene diimide containing polymers (PX–PDIs) as acceptor materials and two polythiophene derivatives (P3HT and PT1) as donor materials were investigated systematically (see picture). The highest power-conversion efficiency (PCE) of all-PSCs was 2.23%, one of the highest PCEs of polymer/polymer blend photovoltaic devices reported to date.

- Thermally Rearranged (TR) Poly(ether−benzoxazole) Membranes for Gas Separation
  Calle, M.; Lee, Y. M. *Macromolecules* **2011**, *44*, 1156–1165.
  Abstract:

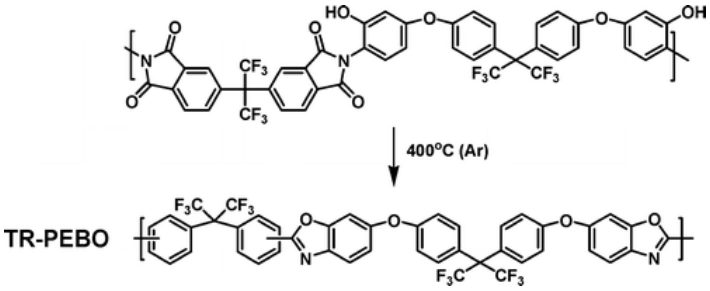

Thermal rearrangement of hydroxyl-containing polyimides in solid state formed microporous polybenzoxazoles showing extraordinarily fast molecular transport for small gas molecules. Their microporous structure and size distribution can be tuned easily by varying the chemical structure of the precursor hydroxyl−polyimide and by using different thermal treatment protocols. This manuscript reports, for the first time, the synthesis of ether containing polybenzoxazole, that is, poly(ether−benzoxazole) (PEBO) membranes by thermal rearrangement of a novel fluorinated poly(*o*-hydroxy ether−imide). The effect of increased chain flexibility on the physical and transport properties of the resultant thermally rearranged (TR) polymer membranes for different thermal treatment protocols (e.g., final temperature and thermal dwell time) have been examined and reported in detail.

- Cyclodextrin-Modified Polyesters from Lactones and from Bacteria: An Approach to New Drug Carrier Systems
  Jazkewitsch, O.; Mondrzyk, A.; Staffel, R. *Macromolecules* **2011**, *44*, 1365–1371.
  Abstract:

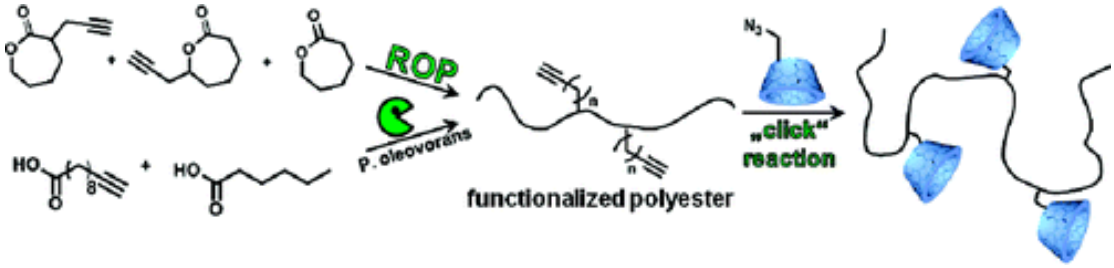

Copper(I)-catalyzed cycloaddition of synthetic and bacterial copolyesters bearing pendant alkyne group with mono-(6-azido-6-desoxy)-β-cyclodextrin was carried out to synthesize β-CD-functionalized copolyester. The synthetic "clickable" copolyesters were obtained by the ring-opening copolymerization of the propargyl-modified lactones and ε-caprolactone. The bacterial copolyesters containing an alkyne group were biosynthesized from a mixture of 10-undecynoic acid and hexanoic acid by the Gram-negative bacteria *Pseudomonas oleovorans*. The modified products of the "click" reaction were characterized by FT-IR, ^{1}H NMR spectroscopy, and DSC. Furthermore, the host guest capability of covalently attached β-cyclodextrin moieties was proved by dynamic light scattering measurements.

- Acyclic diene metathesis: a versatile tool for the construction of defined polymer architectures
  Mutlu, H.; Montero de Espinosa, L.; Meier, M. A. R. *Chem. Soc. Rev.* **2011**, *40*, 1404-1445.
  Abstract:

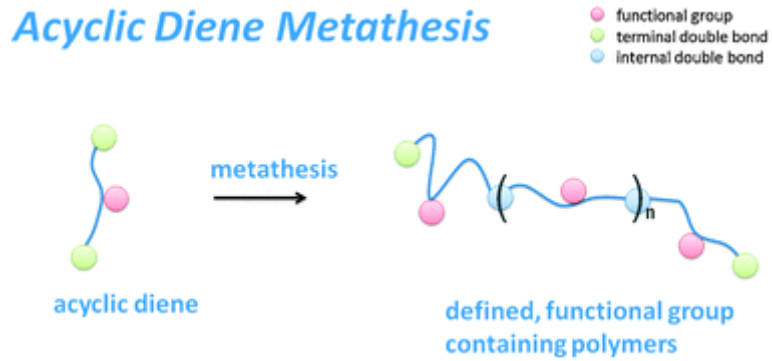

Two decades have passed since the metathesis polymerisation of α,ω-dienes was successfully demonstrated by the group of Wagener and the term acyclic diene metathesis (ADMET) polymerisation was coined. Since then, the advances of metathesis chemistry have allowed to expand the scope of this versatile polymerisation reaction that nowadays finds applications in different fields, such as polymer, material, or medicinal chemistry. This *critical review* provides an insight into the historical aspects of ADMET and a detailed overview of the work done to date applying this versatile polymerisation reaction (221 references).

- Determining association constants from titration experiments in supramolecular chemistry
  Thordarson, P. *Chem. Soc. Rev.* **2011**, *40*, 1305-1323.
  Abstract:

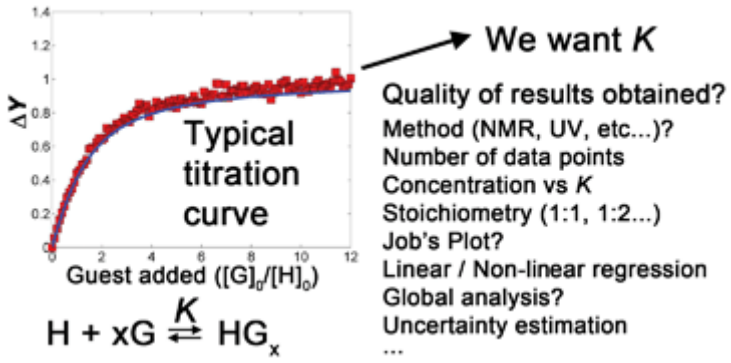

The most common approach for quantifying interactions in supramolecular chemistry is a titration of the guest to solution of the host, noting the changes in some physical property through NMR, UV-Vis, fluorescence or other techniques. Despite the apparent simplicity of this approach, there are several issues that need to be carefully addressed to ensure that the final results are reliable. This includes the use of non-linear rather than linear regression methods, careful choice of stoichiometric binding model, the choice of method (*e.g.*, NMR *vs.* UV-Vis) and concentration of host, the application of advanced data analysis methods such as global analysis and finally the estimation of uncertainties and confidence intervals for the results obtained. This *tutorial review* will give a systematic overview of all these issues—highlighting some of the key messages herein with simulated data analysis examples.